J. Phys. D: Appl. Phys. **32** (1999) 2890–2901. Printed in the UK PII: S0022-3727(99)05645-4

A two-temperature kinetic model of SF_6 plasma

R Girard, J B Belhaouari, J J Gonzalez and A Gleizes

Centre de Physique des Plasmas et de leurs Applications de Toulouse, ESA 5002 Université Paul Sabatier 118 route de Narbonne, F31062 Toulouse Cedex, France

E-mail: jjg@cpa11.ups-tlse.fr

Received 1 July 1999, in final form 10 September 1999

Abstract. Studying the influence of thermal departures from equilibrium in SF_6 circuit-breakers, we develop a two-temperature kinetic model to calculate the composition. Such a kinetic approach has not been adopted until now for SF_6 plasma because of the complexity of chemical processes. Our model takes into account the collisional mechanisms responsible for the creation and disappearance of atoms and molecules through 19 species linked by 66 chemical reactions. To solve the conservation equations, the model uses the direct rates of reactions, that mainly proceed from the literature, and reverse rates, that are computed by two-temperature micro-reversibility laws. Thus, we point out the importance of the choice of the expression of Saha law, comparing Potapov and van de Sanden formulations of this law. We then discuss the impact of thermal departures from equilibrium on plasma composition, on 'mean path' of molecules before dissociation in the plasma, and on the reactions that govern the disappearance of electrons.

Nomenclature

Ca_i	Number of i particles created by unit of time and volume ($m^{-3}\ s^{-1}$)
Da_i	Total disappearance rate for i particles (s^{-1})
D_{AB}	Dissociation energy of molecule AB (J)
d	Mean path (m)
E_i	Ionization energy (J)
K_d	Direct reaction rate
K_i	Reverse reaction rate
n_i	Species i number density (m^{-3})
p	Pressure (Pa)
T_e	Electron temperature (K)
T_{ex}	Excitation temperature (K)
T_h	Heavy particles temperature (K)
Z_I	Partition function of species I
μ_{AB}	Reduced mass of particles A and B (kg)
ν_p^A	Disappearance frequency of species A through reaction 'p' (s^{-1})
ν^A	Total disappearance frequency of species A (s^{-1})
θ	Ratio between electrons temperature and heavy particles one ($\theta = T_e/T_h$)
h	Planck constant (J s)
k_B	Boltzmann constant ($J\ K^{-1}$)

1. Introduction

Models concerning the arc decay in SF_6 circuit breakers have become very sophisticated [1–5]. But in many cases they still fail to predict correctly the success or the failure of the breaking attempt. Actually, simulations appear to lead to a failure of circuit breaking more often than in reality. Many models assume local thermodynamic equilibrium. However, during the extinction there is strong arc blowing, with a high cooling speed ($10^8\ K\ s^{-1}$), leading to very strong phenomena. If the kinetics are not efficient enough chemical departures from equilibrium occur, the populations of chemical species differ locally from the equilibrium composition. These departures could influence the breaking attempt: for example, underpopulation of electrons could appear in critical regions of the arc leading to an increase of the breaking power. Moreover, if the energy transfer between the electrons, that receive the energy through Joule heating, and the heavy particles is not efficient enough, two energy distributions rapidly appear in the plasma, leading to two temperatures (electron temperature T_e and heavy particles temperature T_h). In a previous work [6] we found that taking thermal departures from equilibrium into account leads (in the case of a simplified one-dimensional (1D) model) to a slower cooling of the plasma and thus to a lower breaking power. The discharge energy is trapped by electrons, this energy is progressively transferred to heavy particles during the decay. Thus the local thermodynamic equilibrium hypothesis should be re-examined and two-temperature hydrodynamic models have therefore appeared [7, 8]. This paper concerns the second point which is the departure from thermal equilibrium.

The first aim of this work is to develop a two-temperature composition model which will be able to compute particle densities. There is in the literature a lot of study on SF_6 plasma composition (see e.g. [9–11]), but two-temperature calculations have appeared recently [12–14] to point out the impact of non-equilibrium phenomena on plasma properties, such as electrical conductivity [15]. Another aim of this paper

0022-3727/99/222890+12$30.00

concerns the kinetic mechanisms: we study how thermal departures from equilibrium can act on the composition of the plasma. Moreover, we examine the impact of thermal departures on dissociation of the molecules in the plasma, using a function that we call the 'mean path'. Then we identify the reaction processes that are responsible for the disappearance of electrons, using disappearance frequencies of particles, and we analyse the consequences of thermal departures from equilibrium on these reactions.

2. Model

2.1. Hypotheses

We assume that the energy distribution functions of all species are Maxwellian. The pressure is constant, and the presented results are for $P = 10^5$ Pa. We use a temperature range of 3000 to 12 000 K, which corresponds to the critical temperature range for the arc decay in SF_6 circuit-breakers. Under 3000 K, the electron number density is very low and the resulting electrical conductivity is very small. Further work will consider a decrease of this limit, other reactions will have to be taken into account (e.g. attachment of electrons on SF_x molecules). The 3000 K limitation results from the very long computation time which results from the very sharp variations of SF_x densities below this temperature. To compute the composition above 12 000 K is not determinant, as we only want to investigate the phenomena that occur near current zero. We consider 19 species: e^-, S, S^-, S^+, S_2, S_2^+, F, F^-, F^+, F_2, F_2^+, SF, SF^-, SF^+, SF_4, SF_5, SF_6, SF_2, SF_3. Our choice of these 19 species and 66 reactions results from previous work developed by our team [16–18]. To reduce the computation time for a future study of the extinction, minor species (SF_5^+, SF_4^+, SF_3^+, SF_2^+, F_2^+, $S_2^+ \ldots$) were neglected, as well as negative ions (F_2^-, S_2^-, SF_6^-, SF_5^- and SF_4^-) which can hardly be found over our temperature range. Some authors have taken these negative molecular ions into account [12, 19] but for temperatures greater than 3000 K they found negligible number densities. Most authors (see e.g. [13]) make the same assumptions about the species as us, sometimes they include some exotic species (SSF_2, FSSF, S_2F_{10}), or doubly ionized ions (F^{2+}, S^{2+}), which are present at the highest temperatures (above 12 000 K).

2.2. Equations

The number density of species i is given by its conservation equation (1), where Ca_i and Da_i are the creation and disappearance rates of species i

$$\frac{\partial n_i}{\partial t} + \vec{\nabla}(n_i \vec{v}) = Ca_i - n_i Da_i. \tag{1}$$

In chemical equilibrium conditions there are as many particles i that disappear as are created at the same instant, and the conservation equation reduces to equation (2)

$$n_i = \frac{Ca_i}{Da_i}. \tag{2}$$

The kinetic model solves 19 conservation equations. These equations are not independent. The calculated number densities must also satisfy the perfect gas law, the electrical neutrality and the stoichiometric equilibrium between S and F in the plasma. Thus we only solve 16 conservation equations, the number density of the dominant species comes from Dalton's law, the number density of the dominant charged species is deduced from electrical neutrality, and the number density of the next outstanding species results from stoichiometric equilibrium. The creation and disappearance rates for species i (Ca_i and Da_i) are functions of the direct and reverse rates of all the reactions involving species i. Equation (3) gives the general formulation of one of our 66 chemical reactions. Let us call this reaction p. K_d and K_i are its direct and reverse rates. The chemical equilibrium can be expressed with equation (4).

$$A + B \underset{K_i}{\overset{K_d}{\rightleftarrows}} C + D \tag{3}$$

$$n_A n_B K_d = n_C n_D K_i. \tag{4}$$

The direct rates K_d proceed from the literature and are functions of T_e for electronic attachment reactions and of T_h for dissociative recombination reactions. The reverse rates K_i are computed using microreversibility laws: Guldberg–Waage and Saha laws. In the Guldberg–Waage law (equation (5)) we use T_h as this law concerns molecular reactions

$$\left(\frac{n_A n_B}{n_{AB}}\right) = \frac{Z_A Z_B}{Z_{AB}} \left(\frac{2\pi \mu_{AB} k_B T_h}{h^2}\right)^{3/2} \exp\left(-\frac{D_{AB}}{k_B T_h}\right). \tag{5}$$

The choice of a two-temperature formulation of Saha's law is discussed in the literature: Potapov's formulation (6) [20] was previously the most used [7, 12]

$$n_e \left(\frac{n_{A^+}}{n_A}\right)^{1/\theta} = \frac{2Z_{A^+}}{Z_A} \left(\frac{2\pi m_e k_B T_e}{h^2}\right)^{3/2} \exp\left(-\frac{E_i}{k_B T_e}\right). \tag{6}$$

Equation (6) is written for atomic ions, the partition functions should be raised to the power of $1/\theta$ in the case of molecular ions. Richley and Tuma [21] from a kinetic point of view, showed that the concept of minimum free energy, used by Potapov, is not valid in a multi-temperature plasma. Van de Sanden's formulation (7) [22] was obtained from thermodynamic arguments through the generalization of free energy, and seems to be better for Tanaka *et al* [14] and Han *et al* [23]. We agree with them: the ionization laws must not depend on θ for very low and very high values of n_e [24]; an excitation temperature should be used instead of T_e; and Potapov's formulation fails to predict correctly the density of ionized species at low temperatures (see section 3)

$$\left(\frac{n_e n_{A^+}}{n_A}\right) = \frac{2Z_{A^+}}{Z_A} \left(\frac{2\pi m_e k_B T_e}{h^2}\right)^{3/2} \exp\left(-\frac{E_i}{k_B T_{ex}}\right). \tag{7}$$

This formulation involves the electron temperature T_e and an excitation temperature T_{ex}. The determination of this T_{ex} is still debated. André [12] showed that this temperature has a clear influence on the results. Tanaka *et al* [14] adopted a collisional approach and computed T_{ex} using elastic collision frequencies, which is not correct because T_{ex} depends on inelastic collisions. Gleizes [24] applied kinetic

Table 1. Chemical reaction scheme, rates determined by Arrhenius fit: $K_d = AT^B \exp(-C/T)$.

No	Chemical reaction	Ref.	A	B	C	T	T_{ex}
1	$F^+ + e + e \leftrightarrow F + e$	[9]	5.2×10^{-1}	−1.5	120 230	T_e	T_e
2	$S^+ + e + e \leftrightarrow S + e$		5.2×10^{-1}	−1.5	120 230	T_e	T_e
3	$S + F^- + F \leftrightarrow SF^- + F(\leftarrow)$	[9]	3.92×10^{-12}	0.5	24 950	T_h	T_h
4	$F + S^- + F \leftrightarrow SF^- + F(\leftarrow)$	[9]	3.92×10^{-12}	0.5	40 849	T_h	T_h
5	$S + S^+ + F \leftrightarrow S_2^+ + F(\leftarrow)$	[9]	3.81×10^{-12}	0.5	74 735	T_h	T_h
6	$F + S^+ + F \leftrightarrow SF^+ + F(\leftarrow)$	[9]	3.92×10^{-12}	0.5	43 750	T_h	T_h
7	$F^+ + S + F \leftrightarrow SF^+ + F(\leftarrow)$		3.91×10^{-12}	0.5	44 099	T_h	T_h
8	$F + F^+ + F \leftrightarrow F_2^+ + F(\leftarrow)$		4.09×10^{-12}	0.5	37 020	T_h	T_h
9	$F + F + F \leftrightarrow F_2 + F$	[9]	5.40×10^{-35}	0	0	—	T_h
10	$F + S + F \leftrightarrow SF + F$	[9]	2.80×10^{-34}	0	0	—	T_h
11	$S + S + F \leftrightarrow S_2 + F$	[9]	4.50×10^{-34}	0	0	—	T_h
12	$SF_4 + F_2 \leftrightarrow SF_6$		2.63×10^{-11}	0	7340	T_h	T_h
13	$F_2 \leftrightarrow F + F$	[18]	3.52×10^{-11}	0	16 970	T_h	T_h
14	$SF_5 + F_2 \leftrightarrow SF_6 + F$	[18]	2.63×10^{-11}	0	2438	T_h	T_h
15	$S_2 \leftrightarrow S + S$	[18]	7.95×10^{-11}	0	38 749	T_h	T_h
16	$SF_4 + F \leftrightarrow SF_3 + F_2$	[18]	6.61×10^{-14}	0	1005	T_h	T_h
17	$SF_4 + F_2 \leftrightarrow SF_5 + F$	[18]	2.63×10^{-11}	0	7340	T_h	T_h
18	$SF_4 + F \leftrightarrow SF_5$	[18]	6.61×10^{-14}	0	1005	T_h	T_h
19	$SF_5 + F \leftrightarrow SF_6$	[18]	1.66×10^{-11}	0	0	—	T_h
20	$SF_5 + SF_5 \leftrightarrow SF_4 + SF_6$	[18]	1.66×10^{-11}	0	855	T_h	T_h
21	$S^+ + SF \leftrightarrow S_2^+ + F$	[18]	9.90×10^{-10}	0	0	—	T_h
22	$S^+ + F_2 \leftrightarrow SF^+ + F$	[18]	5.89×10^{-10}	0	0	—	T_h
23	$SF^+ + e \leftrightarrow S + F$	[9]	3.46×10^{-6}	−0.5	0	T_e	T_h
24	$S_2^+ + e \leftrightarrow S + S$	[9]	3.46×10^{-6}	−0.5	0	T_e	T_h
25	$F_2^+ + e \leftrightarrow F + F$	[9]	3.46×10^{-6}	−0.5	0	T_e	T_h
26	$F_2 + e \leftrightarrow F + F + e$		3.00×10^{-10}	0	0	—	T_h
27	$S^- + SF \leftrightarrow S + SF^-$	[29]	3.28×10^{-11}	0.5	0	T_h	T_h
28	$S^+ + S_2 \leftrightarrow S_2^+ + S$	[9]	1.38×10^{-9}	0	0	—	T_h
29	$S^+ + SF \leftrightarrow SF^+ + S$	[9]	1.00×10^{-10}	0	0	—	T_h
30	$F^+ + S_2 \leftrightarrow S_2^+ + F$	[9]	1.66×10^{-9}	0	0	—	T_h
31	$F^+ + SF \leftrightarrow SF^+ + F$	[9]	1.30×10^{-9}	0	0	—	T_h
32	$F^+ + F_2 \leftrightarrow F_2^+ + F$	[9]	6.90×10^{-10}	0	0	—	T_h
33	$F + e + F \leftrightarrow F^- + F(\leftarrow)$	[9]	1.00×10^{-11}	0	40 000	T_h	T_e
34	$S + e + F \leftrightarrow S^- + F(\leftarrow)$	[9]	4.23×10^{-12}	0.5	24 105	T_h	T_e
35	$S^+ + S^- + F \leftrightarrow S_2 + F$	[30]	6.32×10^{-20}	−2.5	0	T_h	T_h
36	$F^- + S^+ + F \leftrightarrow SF + F$	[30]	7.32×10^{-20}	−2.5	0	T_h	T_h
37	$S_2^+ + F^- + F \leftrightarrow S_2 + F + F$	[30]	6.61×10^{-20}	−2.5	0	T_h	T_h
38	$S_2^+ + F^- + F \leftrightarrow SF + F + S$	[30]	6.61×10^{-20}	−2.5	0	T_h	T_h
39	$S_2^+ + F^- + F \leftrightarrow S_2 + F_2$	[30]	6.61×10^{-20}	−2.5	0	T_h	T_h
40	$S_2^+ + F^- + F \leftrightarrow SF + SF$	[30]	6.61×10^{-20}	−2.5	0	T_h	T_h
41	$F_2^+ + F^- \leftrightarrow F + F + F$	[31]	1.50×10^{-7}	0	0	—	T_h
42	$F^+ + F^- + F \leftrightarrow F_2 + F$	[31]	8.18×10^{-20}	−2.5	0	T_h	T_h
43	$F^+ + S^- + F \leftrightarrow SF + F$	[30]	7.30×10^{-20}	−2.5	0	T_h	T_h

considerations on a thermodynamic composition model to build up a law to calculate T_{ex}. To avoid the use of such approximate laws for the computation of T_{ex}, a true kinetic model is needed, which allows the attribution of a T_{ex} for each chemical reaction. From a kinetic point of view, T_{ex} should be equal to T_e or T_h regarding the reaction we consider. If electrons are involved in the reaction $T_{ex} = T_e$, otherwise the reaction is governed by $T_{ex} = T_h$. Electrons receive the discharge energy through Joule heating, they are more mobile and have higher energy than heavy particles. Through collisions electrons transfer some of their energy to heavy particles, they also bring the energy which is necessary to the reaction. Such a method has not been used in SF_6 plasma until now, because of the complexity of chemical processes in this gas. Cliteur [11] recently published a collisional radiative model of composition, but in thermal equilibrium conditions. With our experience of SF_6 kinetics [25], we developed a kinetic model to compute the two-temperature composition. See tables 1–3 for our choice of T_{ex} for each chemical reaction, and for the values and references we used to obtain the direct rates of our 66 reactions. The determination of two-temperature internal partition functions in equations (5) to (7) is also discussed [12, 24, 26, 27], we used values that were previously calculated by our team [10, 28].

To study the impact of departures from thermal equilibrium on the plasma composition, we will have to examine disappearance frequencies and the mean paths of particles. The disappearance frequency of particle A through reaction p is given by relation (8), and the total disappearance frequency of particle A by relation (9).

$$\nu_p^A = K_d n_B \tag{8}$$

$$\nu^A = \sum_{p=1}^{N} \nu_p^A. \tag{9}$$

Table 2. Chemical reaction scheme, rates determined by the Lennard–Jones method: $K_d = A\exp(B + CT + DT^2)\exp(-E/T)$.

No	Chemical reaction	Ref.	A	B	C	D	E	T	T_{ex}
44	$SF_6 + SF_2 \leftrightarrow SF_4 + SF_4$	[18]	5.22×10^{-20}	16.669	1.25×10^{-4}	-8.10×10^{-9}	15 082	T_h	T_h
45	$SF + SF \leftrightarrow F_2 + S_2$	[18]	5.22×10^{-18}	16.549	1.03×10^{-4}	-5.72×10^{-9}	12 468	T_h	T_h
46	$F + SF \leftrightarrow F_2 + S$	[18]	5.22×10^{-18}	16.347	1.50×10^{-4}	-1.07×10^{-8}	22 267	T_h	T_h
47	$F + SF \leftrightarrow SF_2$	[18]	5.22×10^{-18}	16.347	1.50×10^{-4}	-1.07×10^{-8}	0	T_h	T_h
48	$F_2 + S \leftrightarrow SF_2$	[18]	5.22×10^{-19}	16.572	9.99×10^{-5}	-5.34×10^{-9}	5027	T_h	T_h
49	$SF + F_2 \leftrightarrow SF_2 + F$	[18]	5.22×10^{-19}	16.345	1.47×10^{-4}	-1.05×10^{-8}	5027	T_h	T_h
50	$SF + SF \leftrightarrow S + SF_2$	[18]	5.22×10^{-18}	16.549	1.03×10^{-4}	-5.72×10^{-9}	0	T_h	T_h
51	$S_2 + F_2 \leftrightarrow SF_2 + S$	[18]	5.22×10^{-20}	16.654	9.99×10^{-5}	-5.34×10^{-9}	15 082	T_h	T_h
52	$SF_2 + F \leftrightarrow SF_3$	[18]	5.22×10^{-19}	16.473	1.50×10^{-4}	-1.07×10^{-8}	5027	T_h	T_h
53	$SF_2 + F_2 \leftrightarrow SF_3 + F$	[18]	5.22×10^{-20}	16.432	1.47×10^{-4}	-1.05×10^{-8}	15 082	T_h	T_h
54	$SF + F_2 \leftrightarrow SF_3$	[18]	5.22×10^{-19}	16.345	1.47×10^{-4}	-1.05×10^{-8}	5027	T_h	T_h
55	$SF_2 + SF_2 \leftrightarrow SF_3 + SF$	[18]	5.22×10^{-20}	16.669	1.03×10^{-4}	-5.71×10^{-9}	27 421	T_h	T_h
56	$SF_3 + F \leftrightarrow SF_4$	[18]	5.22×10^{-18}	16.567	1.44×10^{-4}	-1.01×10^{-8}	0	T_h	T_h
57	$SF_2 + F_2 \leftrightarrow SF_4$	[18]	5.22×10^{-20}	16.432	1.47×10^{-4}	-1.05×10^{-8}	15 082	T_h	T_h
58	$SF_3 + SF_3 \leftrightarrow SF_2 + SF_4$	[18]	5.22×10^{-18}	16.489	1.44×10^{-4}	-1.01×10^{-8}	0	T_h	T_h
59	$SF_2 + SF_2 \leftrightarrow SF_4 + S$	[18]	5.22×10^{-20}	16.669	1.03×10^{-4}	-5.71×10^{-9}	27 965	T_h	T_h
60	$SF_3 + F_2 \leftrightarrow SF_5$	[18]	5.22×10^{-19}	16.488	1.44×10^{-4}	-1.01×10^{-8}	5027	T_h	T_h

ν_p^A is the product of the direct rate of reaction p and the number density of particle B, with which particle A reacts. In other words ν_p^A is the part of the disappearance rate Da_A which results from reaction p. ν_p^A traduces the relative efficiency of a chemical process to lead to the disappearance of particle A, and can be compared to the other processes involved in its disappearance. Thus we are able to determine the most probable reaction (the outstanding reaction) that govern this disappearance.

The total frequency ν^A is the sum of the N frequencies linked to the N reactions responsible for the disappearance of A. In the following we also use another function, which we call the 'mean path' d: knowing the disappearance frequency of A, and assuming a mean velocity of the plasma as a whole of 10 m s^{-1}, we deduce the distance d (relation (10)), that the particle A can cover in the plasma before being involved in a reaction and disappearing. 10 m s^{-1} is an arbitrary value that helps to figure the relative distances d.

$$d = \frac{v}{\nu^A}. \tag{10}$$

3. Results

3.1. Plasma composition

In the following, we will have to compare the results of our 'kinetic model' to those of 'thermodynamic models'. What we call the 'thermodynamic model', is a classic model, based on the direct resolution of Saha's, Guldberg-Waage's and Dalton's laws. Our kinetic model obtains the densities from the reactions rates (through conservation equations), it also takes Dalton's law into account.

Figure 1 gives the equilibrium composition $\theta = 1$ obtained with our kinetic model and shows the variations of the particle number densities against temperature at atmospheric pressure (10^5 Pa). In order to validate this model, we compared our equilibrium composition with that calculated using a thermodynamic model [10]. We found good agreement between the two series of results and with the results in the literature [9, 12].

Figure 2 presents the composition as a function of T_e, at $P = 10^5$ Pa and for $\theta = 1.5$, this composition was calculated using our kinetic model and the Potapov formulation of the Saha law. This composition is in good agreement with [12], which uses the Potapov formulation in a thermodynamic model.

Figure 3 gives the composition as a function of T_e, for $P = 10^5$ Pa and $\theta = 1.5$, but was obtained using our kinetic model and the van de Sanden formulation of the Saha law, with $T_{ex} = T_e$ to allow comparison with figure 2. The main difference between these two-temperature compositions (figures 2 and 3) is the relative difference between the composition of outstanding charged particles between 3000 and 5000 K, i.e. between F^- and e^- and between S^+ and S_2^+. This can affect the breaking power of the circuit breaker (directly for F^- and e^- because this power depends on the capacity of the plasma to capture the conducting electrons, and through the energy exchange with electrons for S^+ and S_2^+ [6]). We see on figure 3 that F^- becomes the outstanding negative ion under 5000 K, in a similar way as for equilibrium composition. On figure 2, the F^- number density remains negligible. Moreover, computation with the Potapov expression (figure 2) gives an over estimation of S_2^+ density between 6000 to 9000 K

In the following we use van de Sanden's formulation in our kinetic model and we choose T_{ex} from a kinetic point of view: T_{ex} is equal to T_e or T_h regarding the reaction we consider. If electrons are involved in the reaction $T_{ex} = T_e$, otherwise the reaction is governed by $T_{ex} = T_h$. Figure 4 shows the composition obtained with these considerations, at $P = 10^5$ Pa and for a θ of 1.5. It shows very sharp variation of the densities for a critical T_e of about 8000 K, the compositions of the plasmas changes radically in less than 100 K. For temperatures lower than this critical value of T_e, i.e. for a low electron number density, the reactions in the plasma are governed by T_h. Then there is a very fast transition and, for temperatures above 8000 K, i.e. for higher electron number density, reactions are governed by T_e. The critical T_e increases below 1000 K, when θ grows from 1 to 3. Moreover, we found the same behaviour (the existence of a critical T_e and

Table 3. Chemical reaction scheme, other rates: $K_d = A + BT + CT^2 + DT^3 + ET^4$.

No	Chemical reaction	Ref.	A	B	C	D	E	T	T_{ex}
61	$F + e + e \leftrightarrow F^- + e$	[32]	5.32×10^{-31}	-1.15×10^{-34}	1.27×10^{38}	-6.70×10^{-43}	1.35×10^{-47}	T_e	T_e
62	$F + e \rightarrow F^- + h\nu$	[33]	2.53×10^{-15}	-3.46×10^{-19}	3.82×10^{23}	-1.86×10^{-27}	3.37×10^{-32}	T_e	—
63	$S + e \rightarrow S^- + h\nu$	[34]	8.93×10^{-15}	-1.52×10^{-18}	1.51×10^{-22}	-5.30×10^{-27}	0	T_e	—
64	$F_2 + e \leftrightarrow F^- + F$	[35]	1.02×10^{-8}	-4.98×10^{-13}	-3.25×10^{-16}	4.67×10^{-20}	0	T_e	T_e
65	$SF + e \leftrightarrow F^- + S$	[18]						—	T_e
66	$F + F \rightarrow F_2 + h\nu$		-2.87×10^{-23}	9.69×10^{-26}	-2.38×10^{-31}	9.86×10^{-33}	-5.64×10^{-37}	T_h	—

Table 4. Unit of the constant A used in tables 1 to 3.

Chemical reaction	Reaction rate	Unit of A used in the tables
$\alpha_1 + \alpha_2 + \alpha_3 + \cdots + \alpha_j \rightarrow \beta_1 + \beta_2 + \beta_3 + \cdots + \beta_l$	K_d	$\mathrm{cm}^{3(j-1)}\ \mathrm{s}^{-1}$

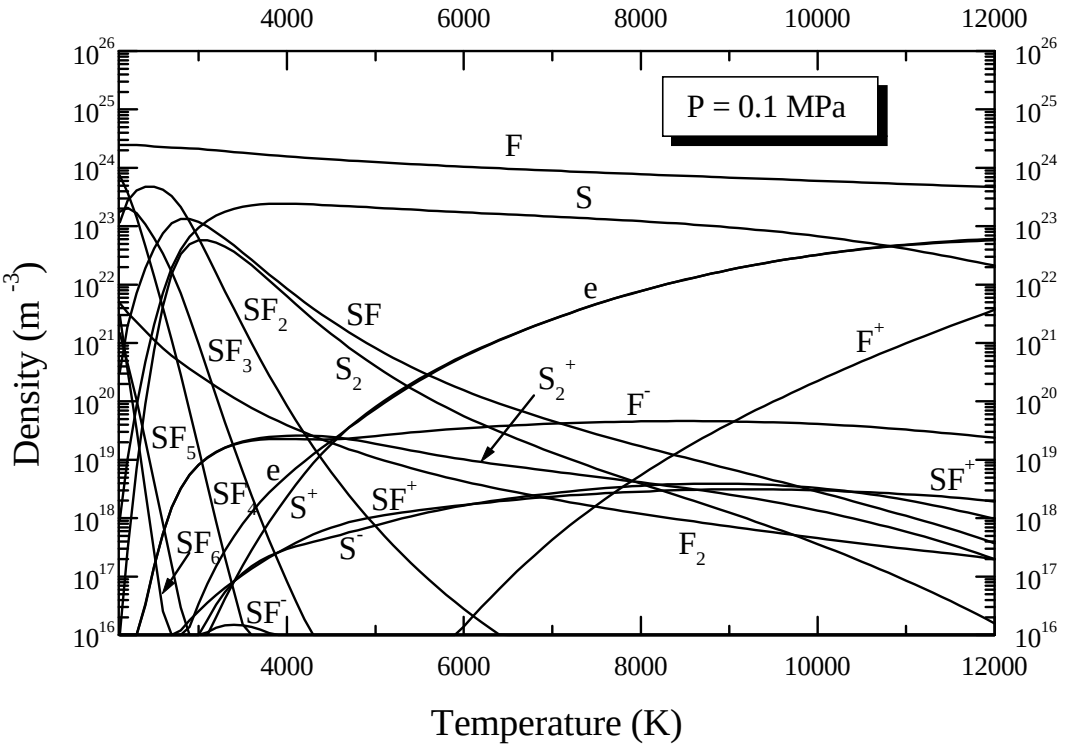

Figure 1. Equilibrium composition of SF_6 plasma.

very sharp variations of the densities) with a thermodynamic composition model when we adapt T_{ex} from T_h to T_e regarding the electron number density [24], and [13–15] reported similar behaviour with another adaptable method. Thus, our two-temperature kinetic model of composition is indirectly validated. These sharp variations may seem unrealistic; in real conditions there are no brutal evolutions of the number densities. However, one must remember that, in thermal non-equilibrium conditions, the value of θ is not constant in the plasma, and that the number densities vary as functions of both T_e and θ (or of T_h, as $\theta = T_e/T_h$). Finally, the obtained variations will be smoother. In his paper, Gleizes [24] illustrates this point, using a 1D arc model: he found a good transition along the plasma radius, from the arc core (where there are very small departures from equilibrium) to its fringes (high departures). Hereafter we will use the composition of figure 4 as our two-temperature composition.

3.2. Mean paths

We now study the 'mean path' of particles in the plasma. This will help us to identify the species which are not immediately dissociated and which could be found in the arc core. Figures 5 and 6 represent the 'mean path', respectively at thermal equilibrium and for $\theta = 1.5$. On both figures 5 and 6 we see that SF_2 molecules are rapidly dissociated for temperatures above 3000 K. SF_x ($x = 1$ to 6) molecules have a low probability of penetrating hot regions. Up to 6000–7000 K, the only molecular species that have a high mean path is S_2, this species is the only molecular species that could enter the arc core through convection without being instantaneously dissociated. A comparison between figures 5 and 6 reveals a translation of the maximums of mean paths to higher temperatures. Thus, S_2 and S_2^+ could be found (and therefore could react to decrease the electron number density) at higher temperatures or deeper in the hot regions. We also see on figure 6

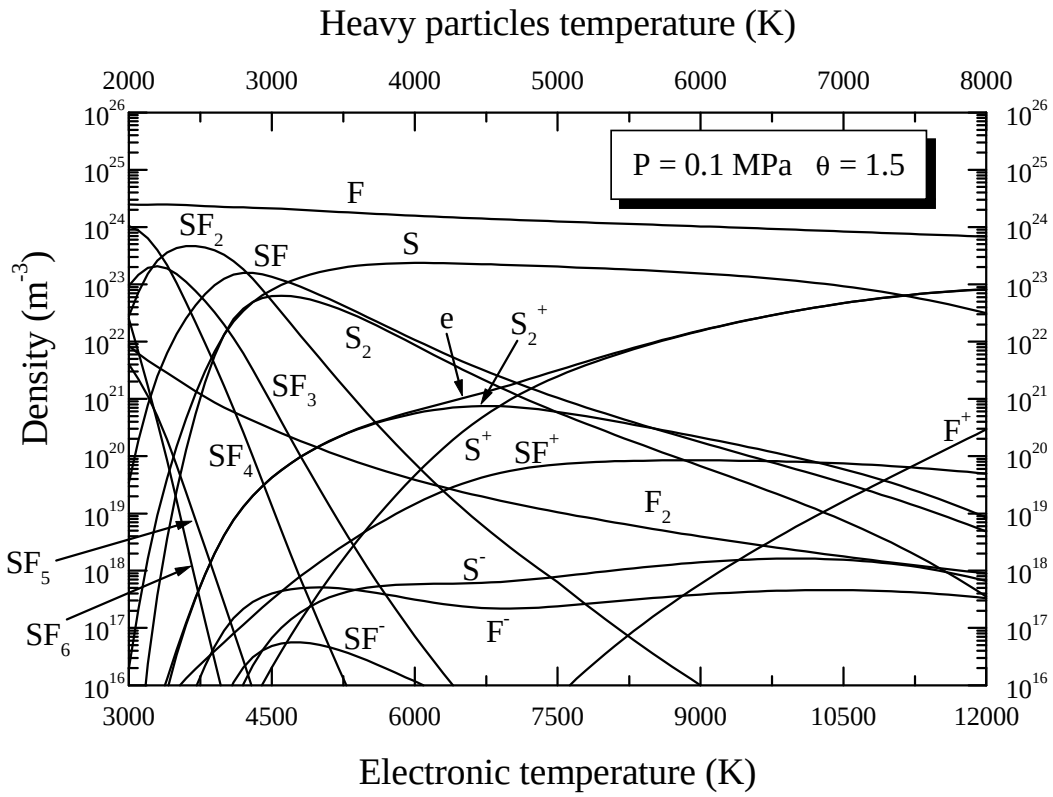

Figure 2. Two-temperature composition calculated using Potapov expression, $\theta = 1.5$.

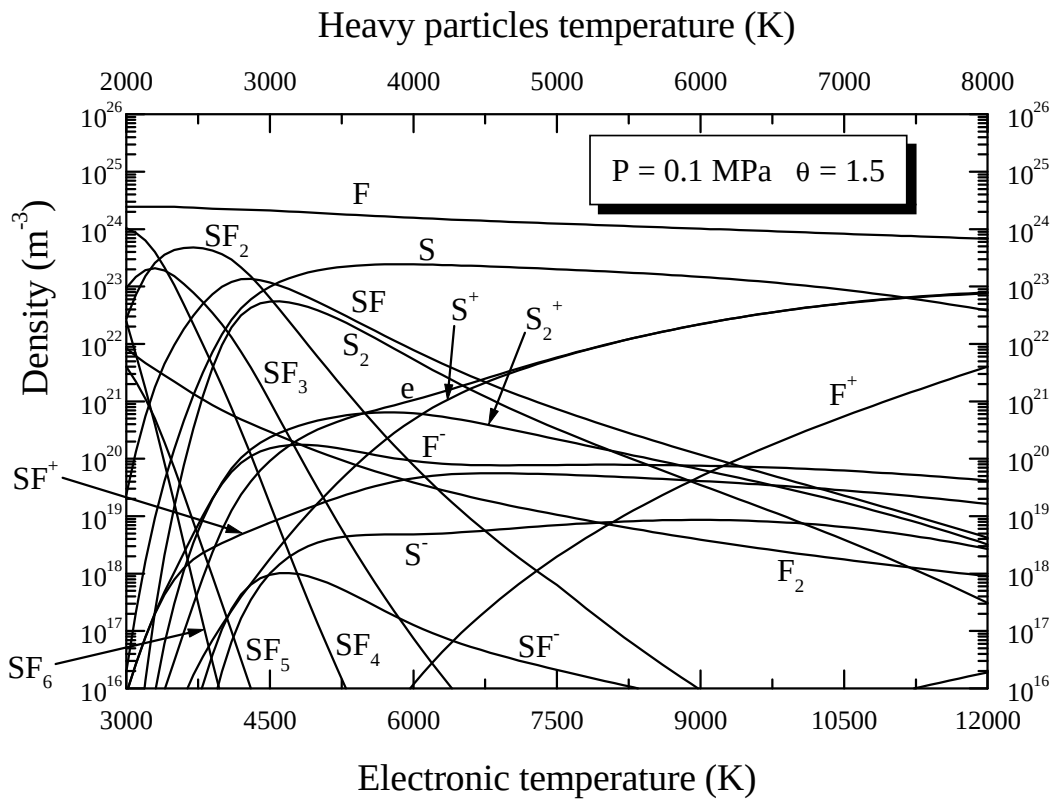

Figure 3. Two-temperature composition calculated using the van de Sanden expression with $T_{ex} = T_e$, $\theta = 1.5$.

a strong change in the mean paths for an electron temperature of about 8000 K. This corresponds to the brutal change of the number densities observed for a threshold electron temperature of about 8000 K on figure 4. For an electron temperature

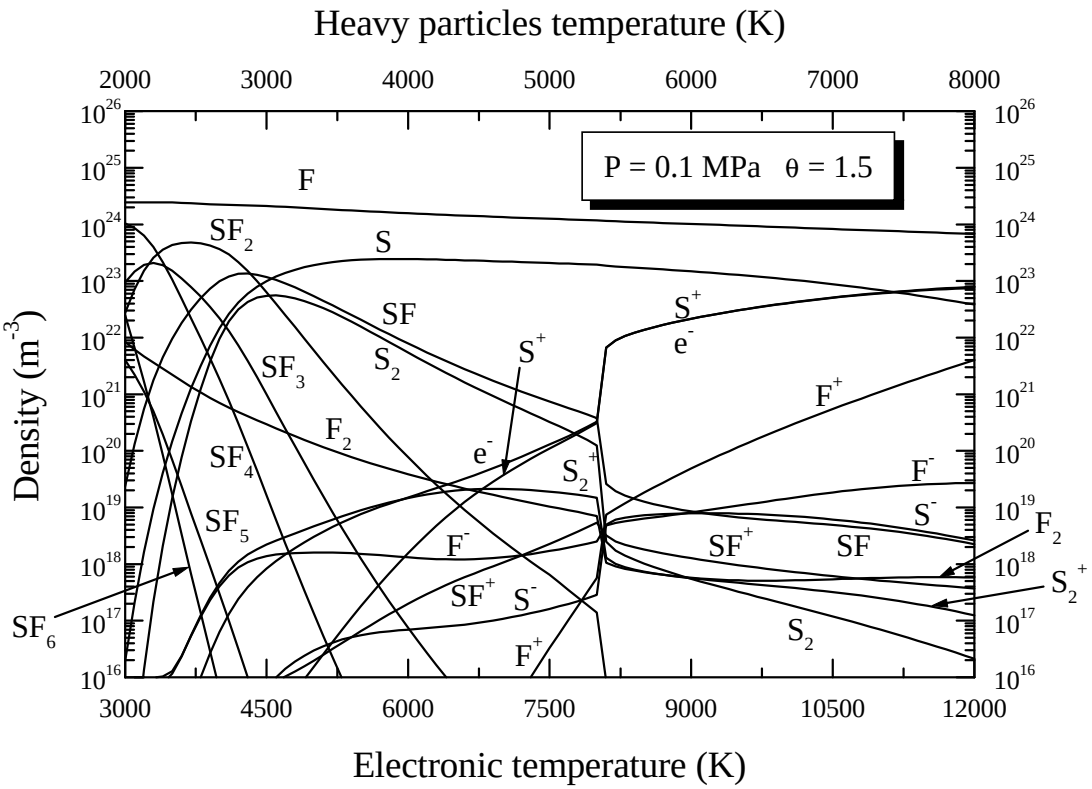

Figure 4. Two-temperature composition of SF_6 plasma, $\theta = 1.5$.

above 8000 K, the mean paths are almost the same as those of equilibrium. At this temperature, molecular species are negligible in the plasma, the reactions that take place involve electrons and are governed by T_e and not by T_h. Mean paths do not depend on θ for T_e greater than 8000 K.

3.3. Disappearance frequencies

Figures 7 and 8 show the contributions of reactions to the disappearance frequency of molecule S_2, respectively at equilibrium ($\theta = 1$) and for $\theta = 1.5$. We see that two reactions are mainly responsible for disappearance of S_2: recombination with F_2 to produce SF (reaction 45) and charge exchange with S^+ to produce S_2^+ (reaction 28). We have shown that S_2 was the only molecular species which could be introduced through convection in the hot regions of the arc. For a T_e between 6500 to 8000 K, S_2 molecules produces S_2^+. When θ increases, the contribution of reaction 45 grows and, up to 8000 K, the contribution of reaction 28 decreases. Thus, at low T_e, production of SF from S_2 is favoured by departures from equilibrium, while production of S_2^+ from S_2 is disadvantaged up to 8000 K.

Figures 9 and 10 present the contributions of reactions to the disappearance of S_2^+, for $\theta = 1$ and for $\theta = 1.5$, respectively. When θ grows, the disappearance of S_2^+ is still governed by reaction 24 for high temperatures, but the temperature range over which this reaction prevails strongly decreases and, up to $T_e = 8000$ K, the disappearance frequency is smaller, there are fewer S_2^+ ions that disappear. Here we found what we have already seen with mean paths: the S_2^+ mean path increases with θ. Moreover, and as identified in equilibrium conditions [25], S_2^+ still disappears through dissociative attachment with electrons at high temperatures.

Figures 11 and 12 show the contributions of reactions to the disappearance frequency of electrons, respectively for $\theta = 1$ and for $\theta = 1.5$. As a whole, the outstanding contributions increase with departures from equilibrium, up to 8000 K. Hence, departures from equilibrium favour the disappearance of electrons. Reactions 65 and 24 still govern the disappearance of electrons between 3000 and 8000 K when θ grows, but dissociative attachment with SF (reaction 65) dominates over a larger temperature range to the detriment of dissociative attachment with S_2^+ (reaction 24). Moreover, we found in our study of S_2 disappearance, that production of SF from S_2 was favoured to the detriment of S_2^+. Therefore, in the two-temperature state, the injection of S_2 by convection, in hot regions, can be responsible for the decrease of electron number densities through the same reactions (28 and 24) as for the equilibrium case [25], but, with high values of θ, other reactions (45 and 65) can interfere. Indeed, this second process involves one main property of SF_6: its electronegativity (through reaction 65 electrons recombines to form F^-).

4. Conclusion

- In order to investigate the impact of thermal departures from equilibrium in SF_6 on the interrupting capability of the circuit breaker, we are developing a two-temperature hydrokinetic model. Therefore, the first aim of this paper was to develop the two-temperature kinetic model, which calculates the composition of SF_6 plasma.

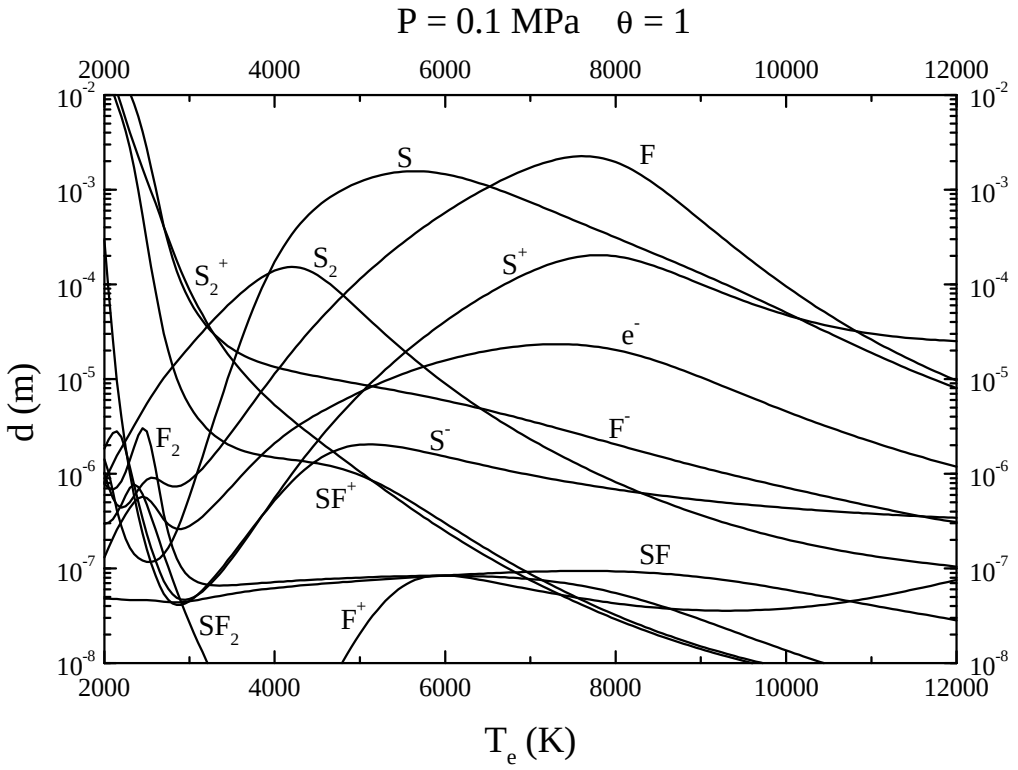

Figure 5. Mean path of particles in the plasma, at thermal equilibrium.

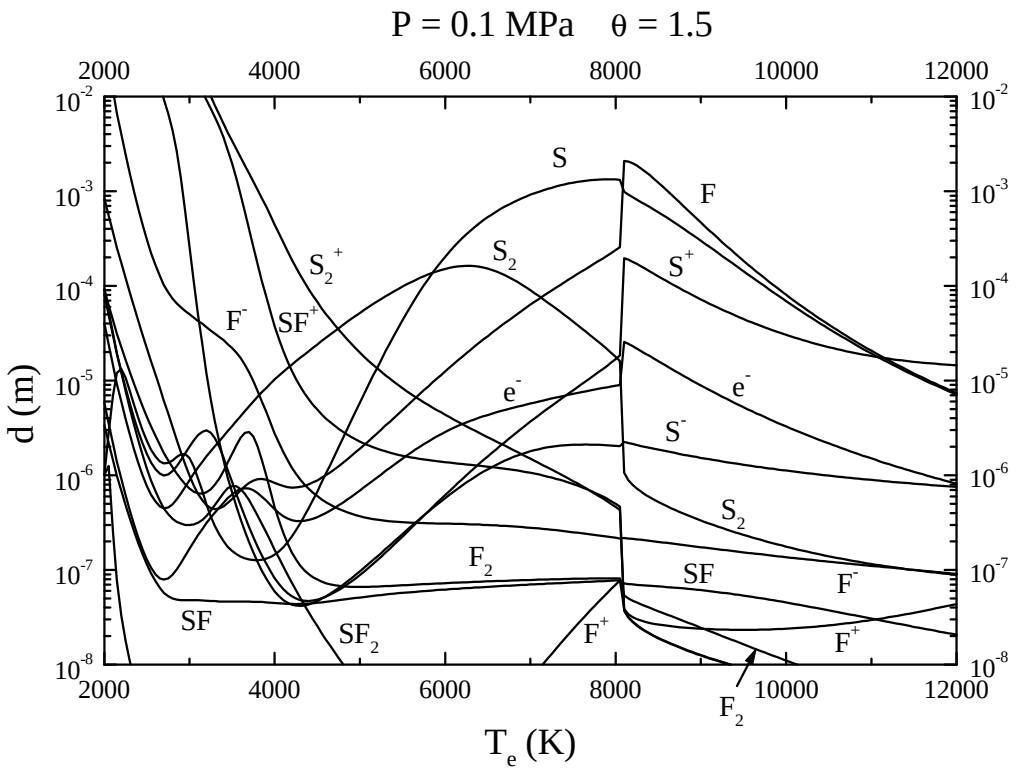

Figure 6. Mean path of particles in the plasma, for $\theta = 1.5$.

- Through the computation of the reaction rates of 66 reactions, we obtain the number densities of 19 species involved in the decomposition of SF_6. This model is not a thermodynamic model, it involves a real kinetic approach and takes the chemical and collisional processes into account.
- In this model the reverse rates of the reactions are calculated by microreversibility, and using van de

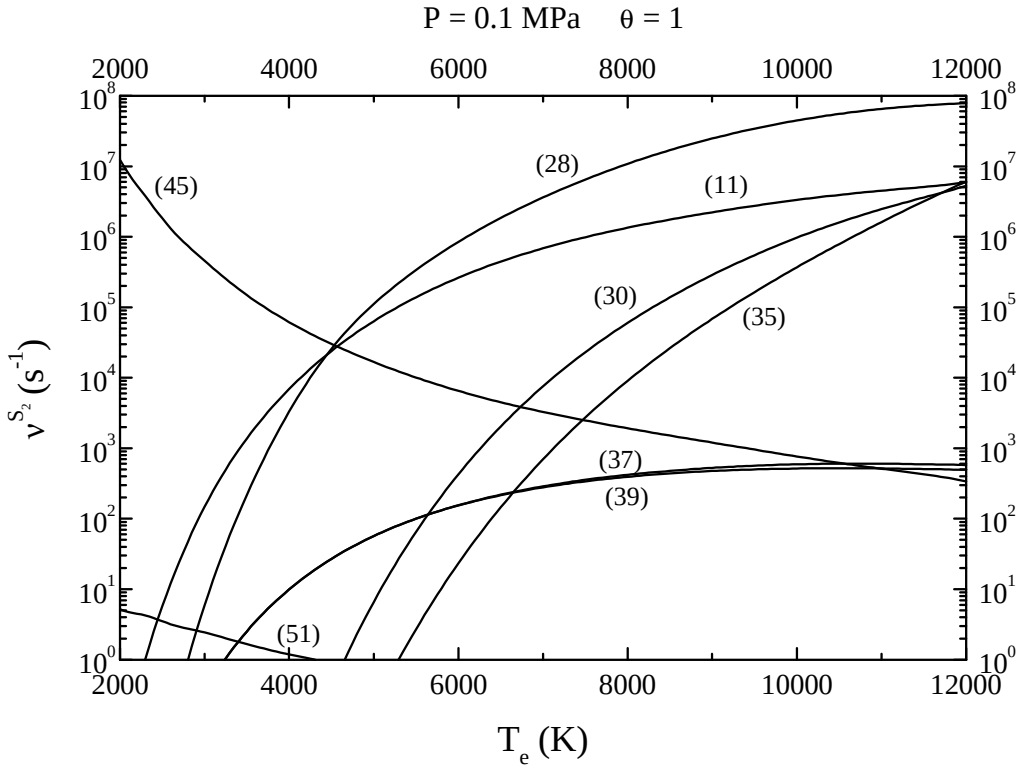

Figure 7. Contributions to the disappearance frequency of S_2, $\theta = 1$.

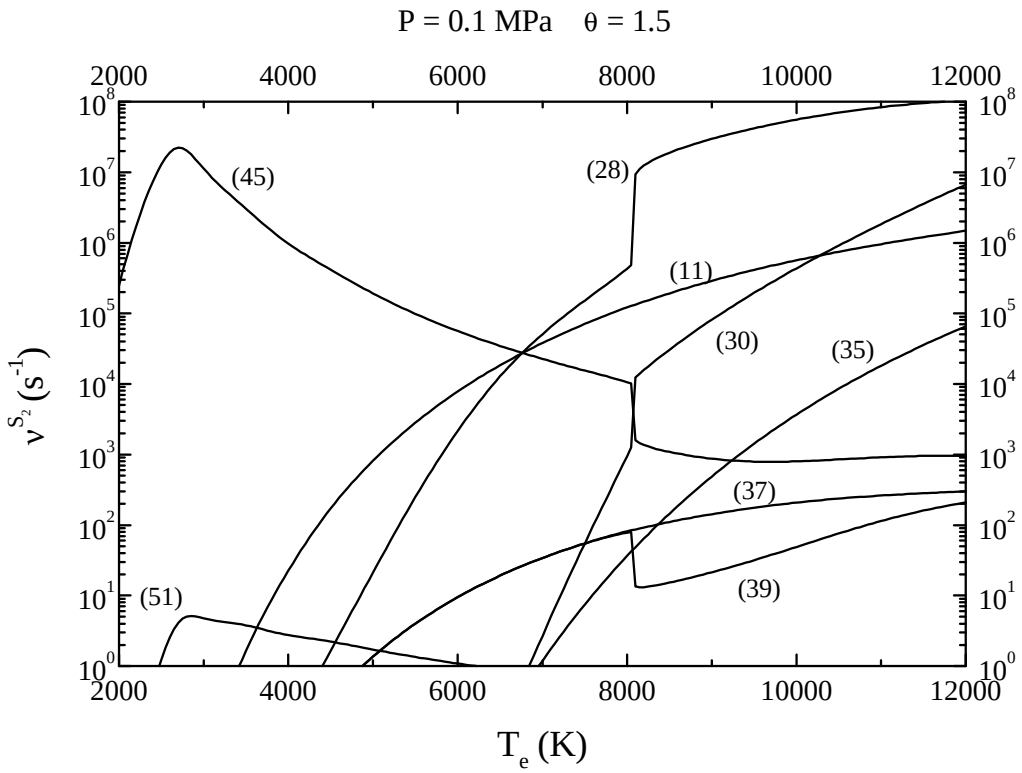

Figure 8. Contributions to the disappearance frequency of S_2, $\theta = 1.5$.

Sanden's formulation of Saha's law instead of Potapov's formulation. For each chemical reaction we choose a T_{ex}, equal to T_e or T_h, whether the reaction involved electrons or not. We found a brutal change of the composition for a T_e of about 8000 K. Studying the reactions that could be responsible for the disappearance of electrons, we show that, at thermal equilibrium or for small values of θ, and in the hot regions of the plasma, S_2

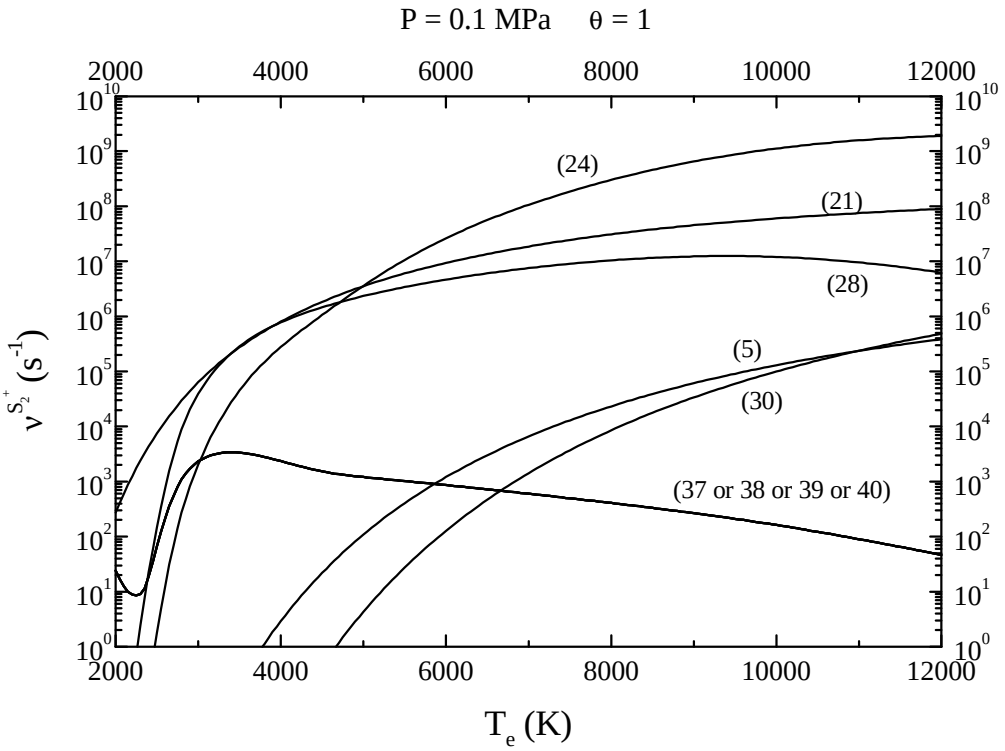

Figure 9. Contributions to the disappearance frequency of S_2^+, $\theta = 1$.

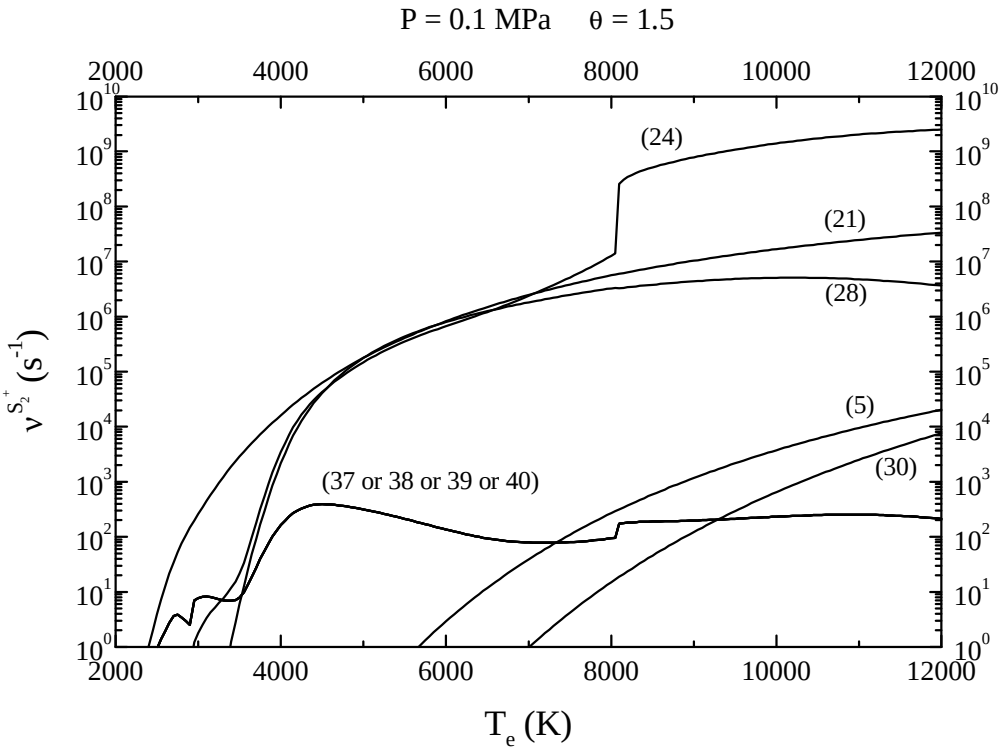

Figure 10. Contributions to the disappearance frequency of S_2^+, $\theta = 1.5$.

molecules produce S_2^+ through charge exchange with S^+, and S_2^+ recombines with electrons. But we also point out that, for high thermal departures, other reactions could interfere: the same S_2 molecules could produce SF, which recombines with electrons to form F^-.

- This study of reactions in the plasma, using the mean path and disappearance frequencies will be very useful to analyse what happens in models of SF_6 plasma. We are now able to determine the line of reactions which is predominant for given temperatures and pressure.

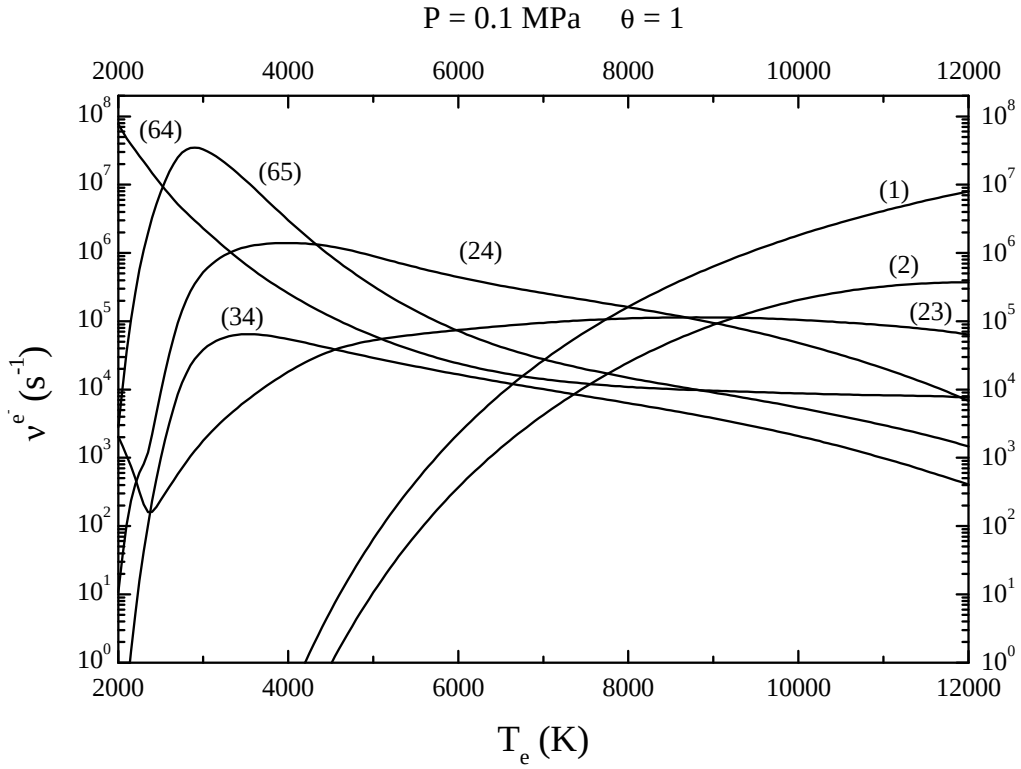

Figure 11. Contributions to the disappearance frequency of electrons, $\theta = 1$.

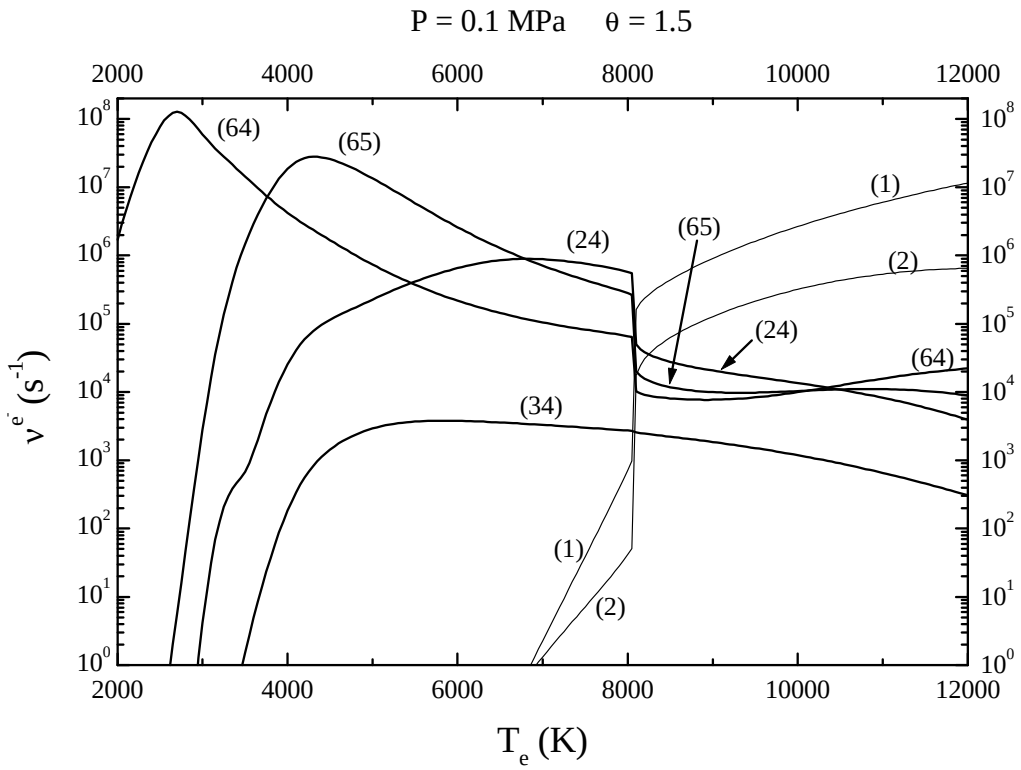

Figure 12. Contributions to the disappearance frequency of electrons, $\theta = 1.5$.

- On the debated subject of microreversibility laws, we recommend the use of van de Sanden's formulation of Saha's law. The kinetic approach allows the choice of a T_{ex} for each chemical reaction.
- We will now use these results for the next step of our study, which is to couple the two-temperature kinetic model we have presented here with hydrodynamic computations. The coupled model will work as follow: the

kinetic part will give reactions rates to the hydrodynamic part, which will use them as source terms of 19 particle conservation equations (equation (1)) to solve each number densities. Hence we will not have to use equation (2) which assumes chemical equilibrium. Thus, we will set up a model of the circuit breaker arc, taking both the chemical and thermal departures from equilibrium into account, with the aim of clarifying SF_6 behaviour close to extinction.

Acknowledgments

This work was partly financed by Electricité de France (EDF) and Alstom T&D.

References

[1] Chevrier P, Barrault M, Fiévet C, Maftoul J and Millon Frémillon J 1997 Industrial applications of high- medium- and low-voltage arc modelling *J. Phys. D: Appl. Phys.* **30** 1346–55

[2] Ciobanu S S, Chévrier P, Fiévet C and Fleurier C 1997 2-D hydrodynamic simulation of a SF_6 arc plasma in an electrical circuit-breaker *12th Int. Conf. on Gas Discharges and Their Applications (Greifswald, 1997)* pp 582–5

[3] Robin-Jouan P, Rathoin S, Serres E, Chevrier P, Barrault M, Fiévet C, Comte A, Boucher T and Vérité J C 1997 Modelling of a two pressure type model of circuit-breaker *12th Int. Conf. on Gas Discharges and Their Applications (Greifswald, 1997)* pp 578–81

[4] Chevrier P, Maftoul J and Rachard H 1997 Hydrodynamic model for circuit breakers design *12th Int. Conf. on Gas Discharges and Their Applications (Greifswald, 1997)* pp 38–41

[5] Kaddani A, Zahrai S, Delalondre C and Simonin O 1995 Three-dimensional modelling of unsteady high-pressure arcs in argon *J. Phys. D: Appl. Phys.* **28** 2294–305

[6] Girard R, Gonzalez J J and Gleizes A 1999 Modelling of a two-temperature SF_6 arc plasma during extinction *J. Phys. D: Appl. Phys.* **32** 1229–38

[7] Krenek P 1987 The two-temperature model of thermal breakdown of SF_6 circuit breaker arc *Acta Techn. CSAV* **6** 667–81

[8] Girard R, Belhaouari J B, Gonzalez J J and Gleizes A 1999 Two-temperature study of a decaying SF_6 arc plasma *13th Symp. on Physics of Switching Arc (Brno, 1998)* pp 5–8

[9] Brand K P and Kopainsky J 1978 Particle densities in a decaying SF_6 plasma *Appl. Phys.* **16** 425–32

[10] Chervy B, Gleizes A and Razafinimanana M 1994 Thermodynamic properties and transport coefficients in SF_6–Cu mixtures at temperatures of 300–30 000 K and pressures of 0.1–1 MPa *J. Phys. D: Appl. Phys.* **27** 1193–206

[11] Cliteur G J, Suzuki K, Paul K C and Sakuta T 1999 SF_6–N_2 circuit-breaker arc modelling around current zero: I. Free recovery simulation using a collisional-radiative plasma model *J. Phys. D: Appl. Phys.* **32** 478–93

[12] André P 1997 Etude d'un plasma de SF_6 hors d'équilibre thermique *J. Physique*, III **7** 1339–59

[13] Tanaka Y, Yokomizu Y, Matsubara T and Matsumura T 1997 Particle composition of two-temperature SF_6 plasma in pressure range from 0.1 to 1 MPa *12th Int. Conf. on Gas Discharges and Their Applications (Greifswald, 1997)* pp 566–9

[14] Tanaka Y, Yokomizu Y, Ishikawa M and Matsumura T 1997 Particle composition of high-pressure SF_6 plasma with electron temperature greater than gas temperature *IEEE Trans. Plasma Sci.* **25** 991–5

[15] Matsumura T, Yokomizu Y, Matsubara T and Tanaka Y 1997 Electrical conductivity and enthalpy of SF_6 plasma in two-temperature state *12th Int. Conf. on Gas Discharges and Their Applications (Greifswald, 1997)* pp 94–7

[16] Mbolidi F 1991 Evolution des densites de particules chargees dans un plasma d'arc d'hexafluorure de soufre (SF_6) en extinction *PhD Thesis* Paul Sabatier University, Toulouse

[17] Gleizes A, Mbolidi F and Habib A A M 1993 Kinetic model of a decaying SF_6 plasma over the temperature range 12 000 K to 3000 K *Plasma Sources Sci. Technol.* **2** 173–9

[18] Borge E 1995 Modélisation de la cinétique chimique d'un plasma d'arc d'hexafluorure de soufre (SF_6) en presence d'impuretés *PhD Thesis* Paul Sabatier University, Toulouse

[19] Chervy B and Gleizes A 1998 Electrical conductivity in SF_6 thermal plasma at low temperature (1000–5000 K) *J. Phys. D: Appl. Phys.* **31** 2557–65

[20] Potapov A V 1966 *High Temp.* **4** 48

[21] Richley E and Tuma D T 1982 On the determination of particle concentration in multitemperature plasmas *J. Appl. Phys.* **53** 8537–42

[22] Van de Sanden M C M, Schram P P J M, Peeters A G, van der Mullen J A M and Kroesen G M W 1989 Thermodynamic generalization of the Saha equation for a two-temperature plasma *Phys. Rev.* A **40** 5273–6

[23] Han P, Chen X and Li H P 1999 On the correct form of the Saha equation for two-temperature plasmas *Chinese Phys. Lett.* **16** 193–5

[24] Gleizes A, Chervy B and Gonzalez J J 1999 Calculation of a two-temperature plasma composition: bases and application to SF_6 *J. Phys. D: Appl. Phys.* at press

[25] Belhaouari J B, Gonzalez J J and Gleizes A 1998 Simulation of a decaying SF_6 arc plasma: hydrodynamic and kinetic coupling study *J. Phys. D: Appl. Phys.* **31** 1219–32

[26] André P, Abbaoui M, Bessege R and Lefort A 1997 Comparaison between gibbs free energy minimization and mass action law for a multi-temperature plasma with application to nitrogen *Plasma Chem. Plasma Proc.* **17** 207–21

[27] Aubreton J, Elchinger M F and Fauchais P 1998 New method to calculate thermodynamic and transport properties of a multi-temperature plasma: application to N_2 plasma *Plasma Chem. Plasma Proc.* **18** 1–27

[28] Chervy B, Gonzalez J J and Gleizes A 1997 Thermodynamic properties and transport coefficients for a two-temperature SF_6 plasma *12th Int. Conf. on Gas Discharges and Their Applications (Greifswald, 1997)* pp 562–5

[29] Christophorou L G 1971 *Atomic and Molecular Radiative Physics* (London: Wiley)

[30] Drawin H W and Emard F 1975 Optical escape factors for bound-bound and free-bound radiation from plasmas *Beitr. Plasma Physik* **15** 273

[31] Wilson J W and Shapiro A 1980 Nuclear-induced excimer fluorescence *J. Appl. Phys.* **51** 2387

[32] Peart B, Forrest R and Dolter K T 1979 Measurements of detachment from F^- by electron impact and test of classical scaling for electron impact detachment cross sections *J. Phys. B: At. Mol. Phys.* **12** L115

[33] Vacquié S, Gleizes A and Sabsabi M 1987 Measurements of the photodetachment cross section of the negative ion fluorine *Phys. Rev.* A **35** 1615–20

[34] Robinson E J and Geltman G 1967 Single- and double-quantum photodetachment of negative ions *Phys. Rev.* **153** 4–8

[35] Corkle D L Mc, Christophorou L G, Christodoulidus A A and Pichiarella L 1986 Electron attachment to F_2 *J. Chem. Phys.* **85** 1966